Structural Eng. / Earthquake Eng. Vol. 6. No. 1, 131s-140s. April 1989
Japan Society of Civil Engineers (Proc. of JSCE No. 404/I-11)

DISTINCT ELEMENT ANALYSIS FOR ROCK AVALANCHE

By Lucia CASAVERDE M., Kazuyoshi IWASHITA**, Yuji TARUMI*** and Motohiko HAKUNO*****

The mechanical behavior of a particle assembly is described based on Cundall's distinct element method which uses an explicit numerical scheme. Particle interaction was detected at every contact, and particle motion modelled for each particle in an assembly.

We used Cundall's simulation method to study the mechanism of slope collapse. Based on results obtained from numerical tests, we conclude that, 1) The shape of the sliding section is wave like, and 2) Particle rotation has a major function in determining the sliding zone of a section.

Keywords: *distinct element method, slope failure, rock avalanche*

1. INTRODUCTION

Soil dynamics can be roughly classified, depending on the idealization of the medium, into continuous and discrete mediums. Handling soil as a continuous body and analyzing it with the finite element method has produced much information. But many unsolved problems remain when considering the soil dynamics of a discrete medium.

Soil, or rock, basically forms a discontinuous medium made up of numerous particles. Phenomena such as rock avalanches and debris flows can be analyzed better by considering rock as a discrete granular assembly; therefore, development of a method by which we can handle rock as a discontinuous medium is necessary.

In the case of a discontinuous medium, soil or rock handling methods can be classified, based on prior studies of soil dynamics into three categories:

① Experiments using actual gravel or granular materials[1].
② Theoretical analyses based on stochastic mechanics[2], and
③ Computer simulations[3].

As to the first category, it is difficult to determine the interior state of an assembly microscopically. There also are several restrictions concerning the principle of similarity. As to the second category theoretical analyses can treat only simple problems. Whereas, as to the third category the model can be analyzed both microscopically and macroscopically by use of various material parameters, e.g., the

* Civil Engineer, Nihon Sekkei Co., Shinjuku, Tokyo, Japan.
** Research Associate, Department of Civil Engineering, Saitama University, Saitama, Japan.
*** Civil Engineer, Japan Highway Public Corporation, Tokyo, Japan.
**** Professor, Earthquake Research Institute, the University of Tokyo, Tokyo, Japan.

frictional coefficient. The limitation on the number of particles and the long computing time needed are the shortcomings of this method;but, new developments in the capabilities of computers are removing such obstacles.

In 1971, the Distinct Element Method (DEM) was introduced by Cundall in which the rock medium was considered an aggregate of elements divided by many discontinuous planes. The method analyzes rock behavior numerically on the assumption that an individual rock element satisfies the equation of motion and the law of action and reaction. Cundall[4),5)] used it to analyze the dynamics of the two-dimensional behavior of a rock particle assembly. Kiyama, Fujimura and Nishimura[6)] later used Cundall's Method to estimate settlement of the ground surface during the construction of a tunnel and assumed that the particles are circular. They also analyzed the behavior of grain particles in a silo during extrusion through a hole[7)].

Hakuno and Hirao[8)] independently established a granular assembly simulation based on circular particles that they used to study the static deformation of sand. Because of the time required to compute the equations for all the particles simultaneously, only the static problem could be solved.

Uemura and Hakuno[9),10)] modified Cundall's method by introducing a restitution coefficient and made a dynamic analysis of a soil model having more than 3000 circular elements with different radii.

Use of circular elements saved CPU time. A rock avalanche could be analyzed successfully by this method as described in the following sections.

2. CUNDALL'S DISTINCT ELEMENT METHOD

(1) Distinct element method

The motion of a particle having the mass, m_i, and the moment of inertia, I_i is

$$m_i\frac{d^2U}{dt^2}+C_i\frac{dU}{dt}+F_i=0 \quad \cdots\cdots (1)$$

$$I_i\frac{d^2\varphi}{dt^2}+D_i\frac{d\varphi}{dt}+M_i=0 \quad \cdots\cdots (2)$$

in which F_i is the sum of all the forces acting on the particle,

M_i is the sum of all the moments acting on it,

C_i and D_i are the damping coefficients,

U is the displacement vector, and φ is the angular displacement.

The following modifications were made to Cundall's DEM :

1) We introduced a restitution coefficient for when a particle collides with other particles.

2) We introduced the coefficient of rotation control of a particle.

If the angular velocity $V_\varphi(\mathrm{I})=0$;
and the moment $|\mathrm{FM}\ (\mathrm{I})|$, when
DFM is a fixed value of the moment that controls rotation, then $|\mathrm{FM}(\mathrm{I})|=0$ means that there is no rotation.

(2) Particle elements

The displacement of a particle can be obtained by integrating eqs. (1) and (2). An elastic spring between particles must be introduced in order to estimate the force produced by the contact of other particles acting on a certain particle. The acting force can not be estimated by the law of the equilibrium of force alone : Particle deformation also must be considered for three or more particles coming into contact. We assumed two types of elastic springs and dampers. One for the normal force and one for the shear force (Fig. 1 (a), (b)).

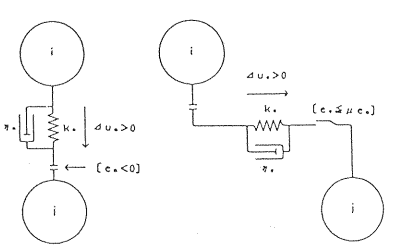

(a) normal direction (b) tangential direction

Fig. 1 Elastic Spring and Viscous Dashpot.

3. SIMULATION OF A ROCK AVALANCHE

Large scale slope collapse occurred in Japan at the time of Nagano Prefecture Seibu earthquake of 14 September 1984. On 5 march 1987 many slopes collapsed because of an earthquake at Mt. Reventador in Ecuador. Many examples of slope collapse also have been recorded following other earthquakes.

The amount of pore water between rock particles has a great effect on whether a slope will collapse;but, for simplicity we have not taken pore water into consideration in this research.

(1) Model of the particle assembly

We constructed a model of a particle assembly that had diameters of lognormal distribution. The radii of particles are in the range of 3 m to 15 m. Development of the packing of our assembly model was not easy because of the large number of particles present and the great height from which they were dropped. In simulating the packing we found that when the number of particles increase, the time step as well as the elastic coefficients for the walls, those for the elements and the coefficient of restitution have important

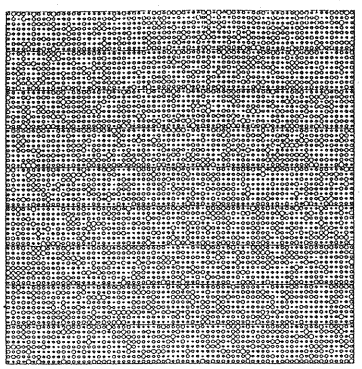

Fig. 2 Initial Positions for the Packing of 5040 Particles.

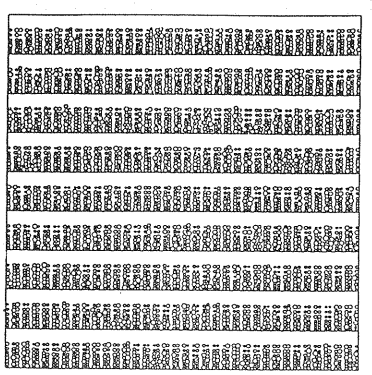

Fig. 3 Results after Step One of the Packing Process.

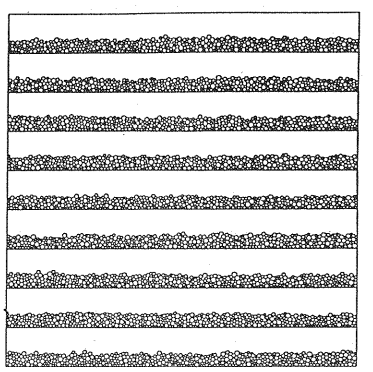

Fig. 4 Partial Result when packing by parts.

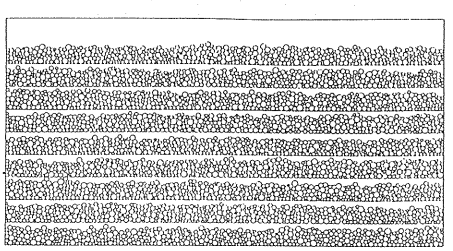

Fig. 5 Results of Approximating Boxes then Removing Intermediate Floors.

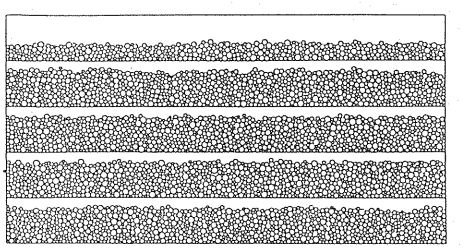

Fig. 6 Results of Packing the Sample Shown in Fig. 5.

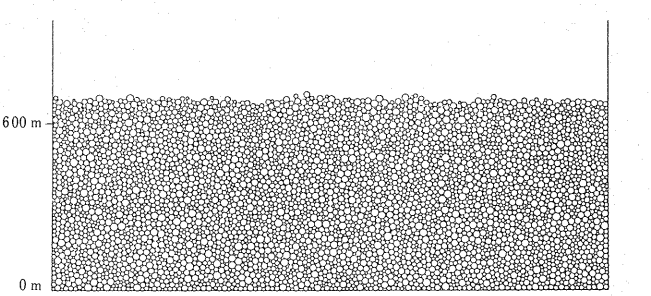

Fig. 7 Final Results of the Packing of 5040 Particles.

effects. Packing was done by dropping the particles from an initial position. Potential energy was generated because of dropping an increased number of particles from a very high elevation.

In order to deal with this potential energy, we developed a method by which packing was done in segments.

(2) Packing 5040 particles

Because of the large number of particles used, we developed a method of packing by segments that basically deals with an assembly enclosed in a box. We divided the particles into nine groups of 560 particles each (Fig. 2), then we packed these nine groups separately (i.e. simulating nine independent boxes) at the times shown in Figs. 3 and 4. Once this was done we set these boxes filled with particles closer to together, in order to avoid great heights. Afterwards we removed the intermediate floor between each part of boxes, which gave us four boxes of 1120 particles each. The last one box had 560 particles (Fig. 6). We again packed these groups to obtain a larger assembly. This procedure was repeated four times until we obtained the final assembly configuration (Fig. 7).

4. TESTS WITH 1089 PARTICLES

Various tests were necessary to determine the numerical values of the elastic and damping coefficients, as well as those of the friction coefficients and the values of the control moment and of cohesion in order to establish a stable numerical process.

The effects of the foregoing parameters on the mechanical process was studied after taking off the right wall of each box in which the particles were enclosed. In another instance, the assembly was cut so that it simulated the slope of Mr. Ontake. These tests were made to determine the mechanical process that

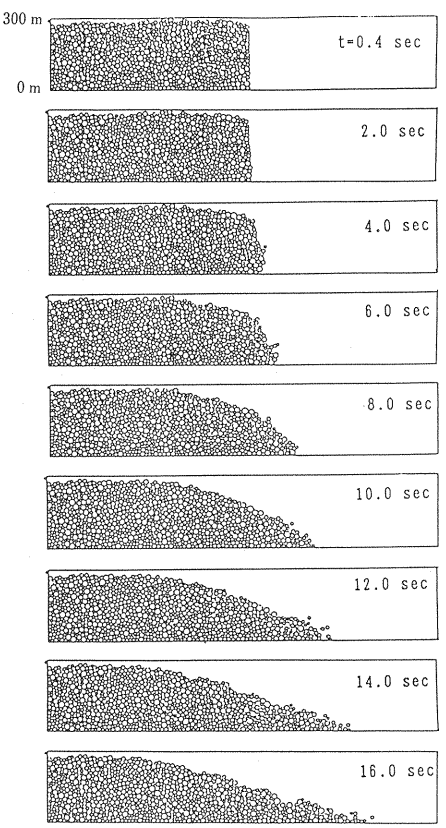

Fig. 8 Particle Distribution when QWD=0.5.

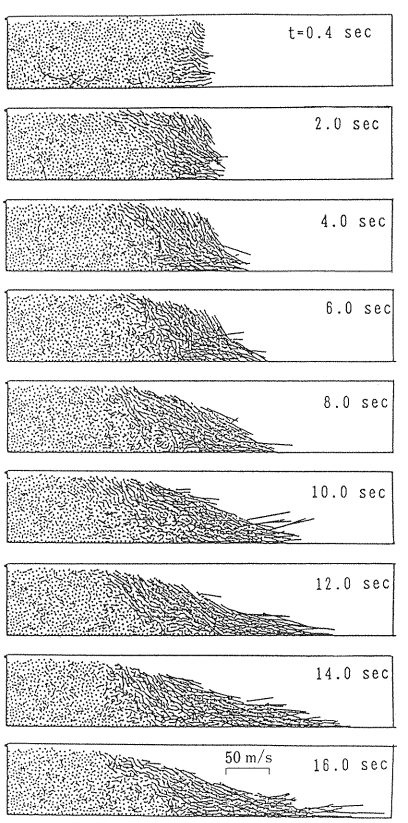

Fig. 9 Velocity Distribution when QWD=0.5.

Table 1 Simulation Data.

QKN	$9.00*10^8$	QWN	$9.00*10^8$
QYN	$1.40*10^7$	QZN	$1.40*10^7$
QKS	0.00	QWS	0.00
QYS	0.00	QZS	0.00
QD	0.0	Δt	0.005
QS	0.00	ρ	$2.20*10^3$
QWD	0.00	DFM	0.00
QE	0.10	DFC	0.00
		QWV	0.00

Table 2 Explanation of Coefficient Data.

QKN	Elastic Spring Coefficient of a Particle in the Normal Direction (KN/m)
QYN	Damping Coefficient of a Particle in the Normal Direction (KN·s/m)
QKS	Elastic Spring Coefficient of a Particle in the Tangential Direction (KN/m)
QYS	Damping Coefficient of a Particle in the Tangential Direction (KN·s/m)
QD	Sliding Friction Coefficient of a Particle
QS	Static Friction Coefficient of a Particle
QWD	Sliding Friction Coefficient of the Wall
QE	Restitution Coefficient
QWN	Elastic Spring Coefficient of the wall in the Tangential Direction (KN/m)
QZN	Damping Coefficient of the Wall in the Normal Direction (KN·s/m)
QWS	Elastic Spring Coefficient of the Wall in the Tangential Direction (KN/m)
QZS	Damping Coefficient of the wall (KN·s/m) in the Tangential Direction
Δt	Interval for the Calculation (s)
ρ	Density of the Particles (Kg/m^3)
DFM	Initial Resistant Moment of Rotation of a Particle (KN·m)
DFC	Cohesion of the Particles (KN)
QWV	Damping Coefficient for the Rotation of a Particle

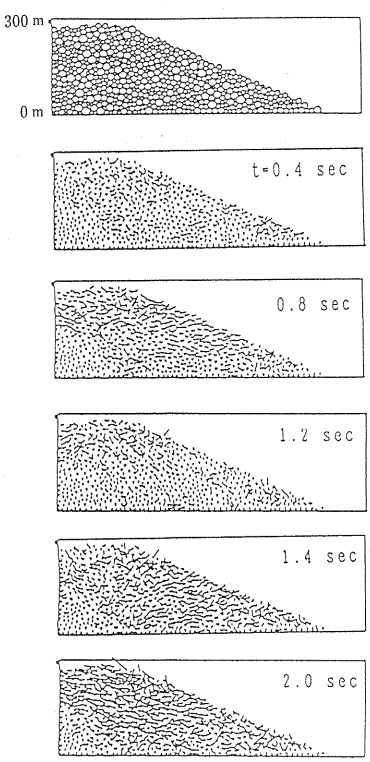

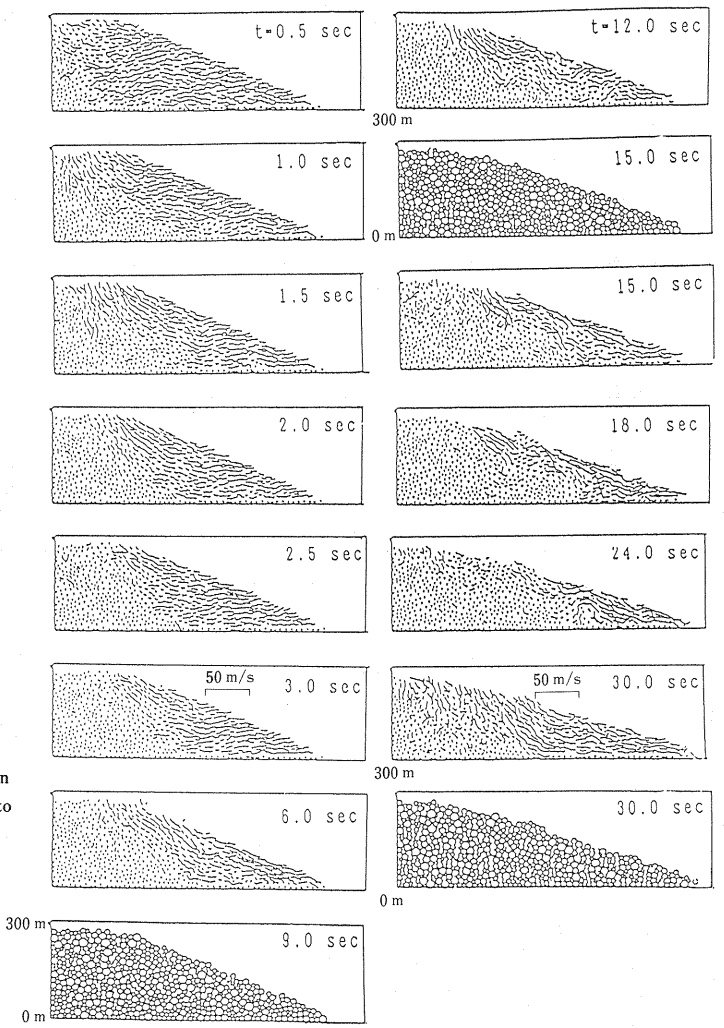

Fig. 10 Velocity and Particle Distribution when the Sample was subjected to Sinusoidal Input Motion.

Table 3 Simulation Data.

QKN	$9.00*10^8$	QWN	$9.00*10^8$
QYN	0.00	QZN	$1.40*10^7$
QKS	$2.30*10^8$	QWS	$2.30*10^8$
QYS	0.00	QZS	$3.50*10^6$
QD	1.00	Δt	0.001
QS	1.00	ρ	$2.20*10^3$
QWD	1.00	DFM	$3.28*10^7$
QE	0.10	DFC	$3.60*10^8$
		QWV	$3.00*10^8$

Fig. 11 Velocity and Particle Distribution over a 30-Second period When the Sample was Subjected to Input Motion for 0.5 s Duration.

operates when a slope assembly is subjected to different input motions.

(1) Development of the mechanical process after removing the right wall of a box

This test was done with a loose assembly without damping in the angular velocity (i.e., no controlling rotation). The model consists of particles with radii from 3 m to 15 m. In Figs. 8, and 9 the case in which the sliding friction coefficient is QWD=0.5 is shown, for which it is possible to observe the movement process for up to 16 seconds. The input parameters used are given in Table 1. The results of this test show that the surfaces of the sliding particles gradually change shape with time.

(2) Subjection of the slope assembly to input motion

For 2 seconds, the sample was subjected to sinusoidal input motion that had an acceleration of 0.5 G and a frequency of 0.5 Hz. The values of the parameters used are shown in Table 2. In Fig. 10(a), the mechanism of the movement of the assembly for 2 seconds (equal to the input duration) is shown. This figure clearly indicates how the orientation of the velocity distribution is changed when the sine wave is negative (at 1.2 second) and its leftward direction at the end of the input motion (2 seconds). The sample then was subjected to a half sine motion of maxmum acceleration equal to 1G with a frequency of 0.5 Hz and a duration of 0.5 second. Fig. 11, 12 and 13 show the movement of the sample, as well as the shear force distributions.

The velocity distribution shows the development of the movement of the assembly. At 0.5 second, just after the shock motion, almost all the particles had begun to move forward. The 3rd second (2.5 seconds after the shock), clearly shows how the sliding section developed. With time, sliding continued to develop and the sliding section took on a wave shape. There is a marked change in the shear force distribution during the 30 seconds studied. The maximum shear force at 0.5 second was $188.7*10^3$ kN, 7 times the shear

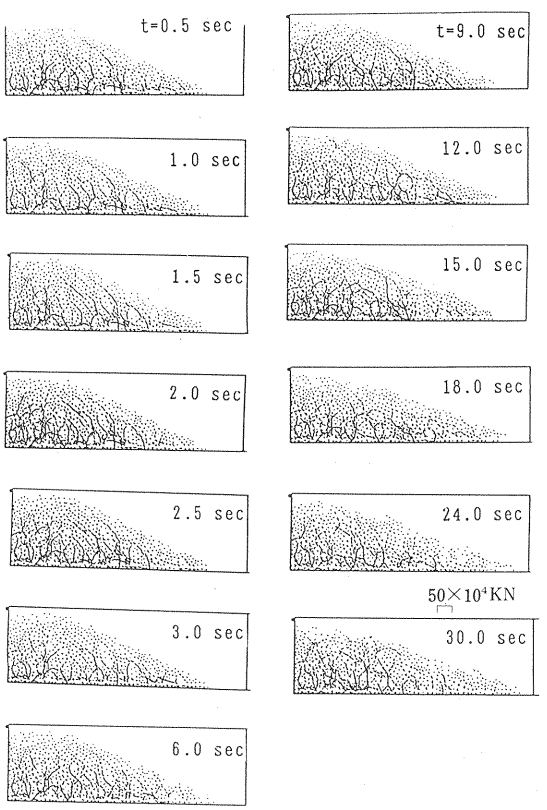

Fig. 12 Normal Force Distribution for 30 seconds When the Sample was subjected to Input Motion of 0.5 s Duration.

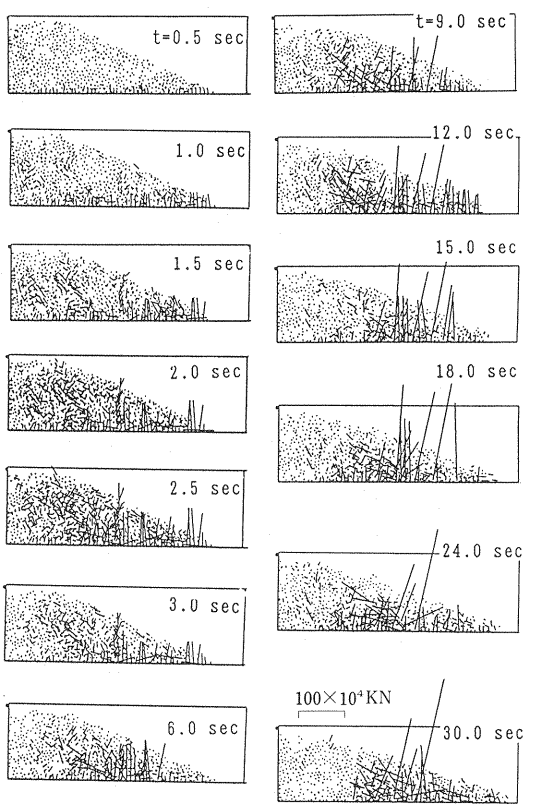

Fig. 13 Shear Force Distribution for 30 Seconds When the Sample was subjected to Input Motion of 0.5 s Duration.

force in the static condition. The maximum shear force at the 30 th second was 282.5*10⁴ kN, 100 times the shear force in the static condition.

If the shear force and velocity distributions are compared (e. g., at the 12 th second), the shear forces are seen to be greater around the sliding section. But, at the 30 th second, it is clear that in the upper part of the assembly some particles are still in motion. This is because the shape of a particle is circular;therefore, rotation comes to have an important role. In the case of real soil, its particles are irregular so that they can not so easily rotate as in the case of circular particles.

5. A LARGE SAMPLE SUBJECTED TO INPUT MOTION

Table 4 Simulation Data.

QKN	$9.00*10^8$	QWN	$9.00*10^8$
QYN	0.00	QZN	$1.40*10^7$
QKS	$2.30*10^8$	QWS	$2.30*10^8$
QYS	0.00	QZS	$3.50*10^6$
QD	0.20	Δt	0.001
QS	1.00	ρ	$2.20*10^3$
QWD	1.00	DFM	$3.28*10^7$
QE	0.10	DFC	$9.00*10^6$
		QWV	$3.00*10^9$

The input motion used is a half sine motion with a maximum acceleration equal to 1.0 G and a frequency of 0.5 Hz. The duration of this motion was 0.5 sec. The input parameters used to produce it are given in Table 3.

(1) Test results (velocity distribution)

Movement development is shown in Fig. 14 for an input motion lasting 0.5 second. Observation of the velocity distribution at this step, shows that when the assembly is first subjected to the input motion, all the particles move randomly. As time passes, ordered movement begins. At t =0.4 sec, the particles begin moving forward. Concerted movement forward is present at t=2.0 sec (0.9 second after the input motion) Fig. 15.

(2) The role of particle rotation

The situation at t=38.0 sec is shown in Fig. 16. The sliding zone is clearly shown at the velocity

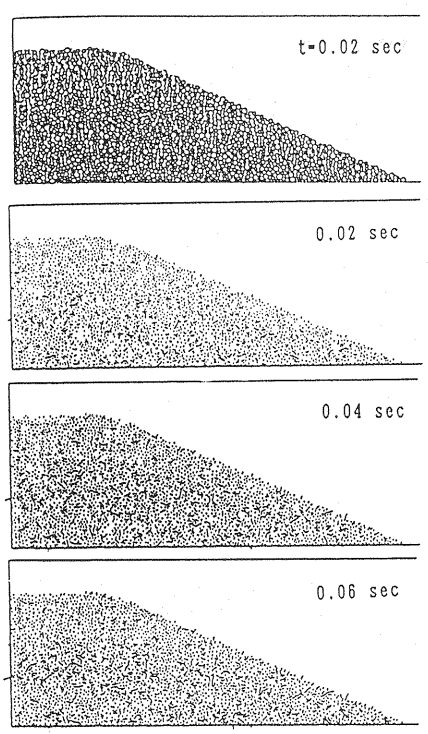

Fig. 14 Particle and Velocity Distributions When the Sample was Subjected to Input Motion (t : 0.02–0.06 s).

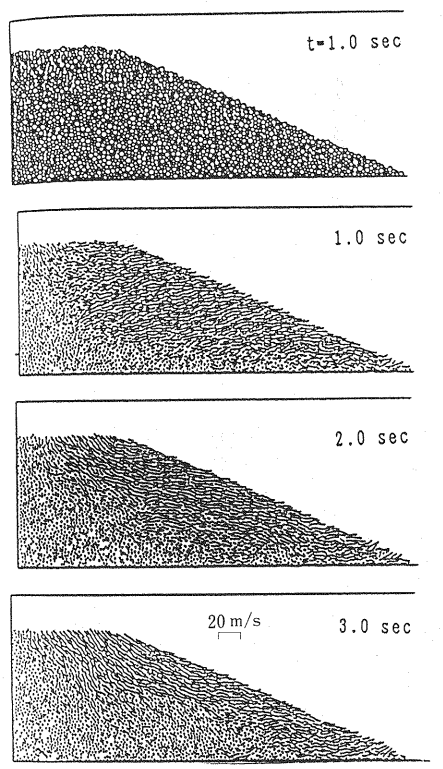

Fig. 15 Particle and Velocity Distributions When the Sample was Subjected to Input Motion (t : 1.0–3.0 s).

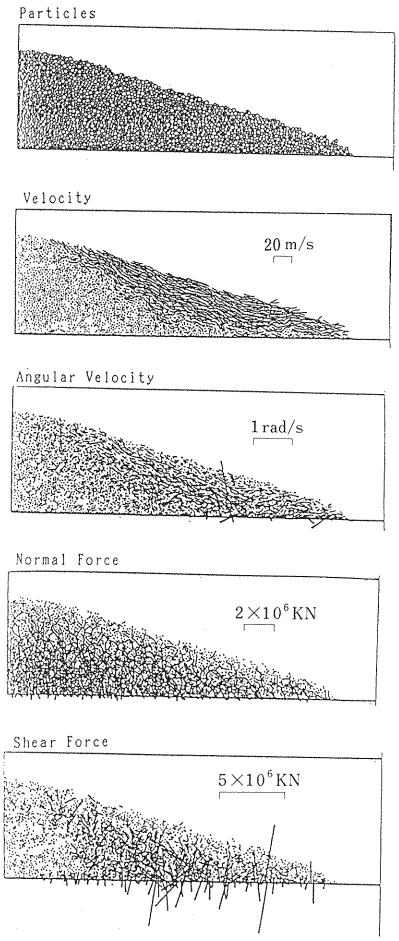

Fig. 16 Assembly Response When the Sample was Subjected to Input Motion Lasting 0.5 s (t=38.0 s).

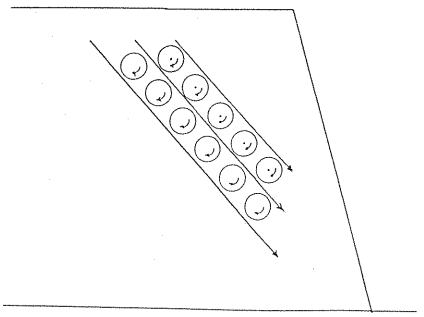

Fig. 17 Role of Particle Rotation in the Slope Slide.

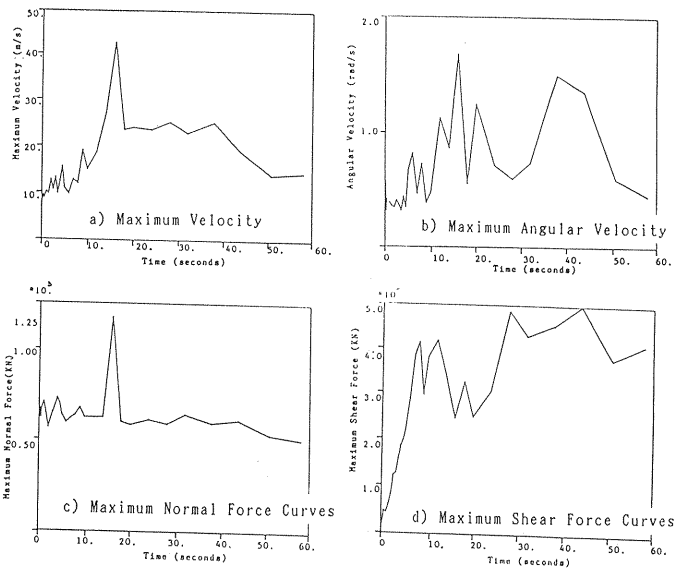

Fig. 18 Time Histories of Maximum particle Response.

distribution because the zone with no velocity does not slide. The angular velocity (rotation) has its value around at the border region between the sliding and non-sliding. Therefore, Fig. 16 shows that the rotation of the paricles (angular velocity) has an important function in the process of land slide (Fig. 17). The illustration of angular velocity in Fig. 16 is made so that the vector length indicates the angular velocity and the vector orientation coincides with the particle velocity.

(3) Graphic displays for 58 seconds

The curves of the maximum velocity, the maximum angular velocity, the maximum normal forces and the maximum shear forces over a period of 58 seconds for 0.5 sec of input motion are given in Fig. 18 (a) - (d). The maximum velocity shows sharp fluctuations and reaches its peak value early, by 20 seconds after applying the input motion. The velocity begins to slow at 38.0 sec. The maximum normal force remains relatively constant for the 58-second period studied except from 16 sec to 18 sec. The maximum shear force shows very large values in comparison to its beginning values.

(4) Particle paths

To trace the path of the movement we selected 16 particles at random from the 3 162-particle assembly (Fig. 19). Fig. 20 displays the paths of these 16 particles for an input motion lasting 0.5 sec. Groups (a) and (b) correspond to particles present in the internal part of the assembly, most of which correspond to

group (a). Particles P 1, P 5 and P 10 do not move. Particle P 30 moves because of its location towards the outer part of the assembly, possibly because it was in an area in which internal movement developed. Group (b) contains particles situated more toward the outer part of the assembly;therefore, they move.

Groups (c) and (d) correspond to particles located in the outer most part of the assembly. For both groups the paths traversed are longer because these particles are situated in the sliding area of the assembly that was subjected to the input motion.

Group (c) is composed of those particles located at the top of the surface slope.

Group (d) is composed of those particles situated at the bottom of the surface slope.

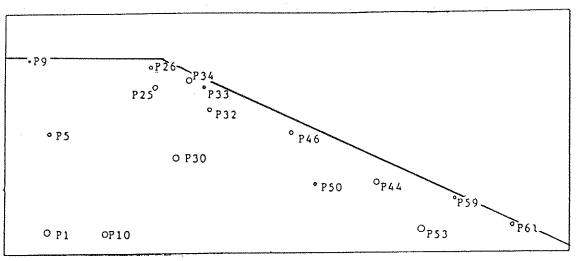

Fig. 19 The 16 Particles Selected for Path Tracing.

Table 5 Data for Sample Particles.

	Group (a)				Group (b)			
Radius (M)	11.61	7.04	10.79	11.43	4.35	9.37	10.21	12.36
Particle	P 1	P 5	P 1 0	P 3 0	P 9	P 2 5	P 5 0	P 5 3
	Group (c)				Group (d)			
Radius (M)	6.90	7.72	5.71	10.87	5.95	7.54	6.47	7.4
Particle	P 2 6	P 3 2	P 3 3	P 3 4	P 4 4	P 4 6	P 5 9	P 6 1

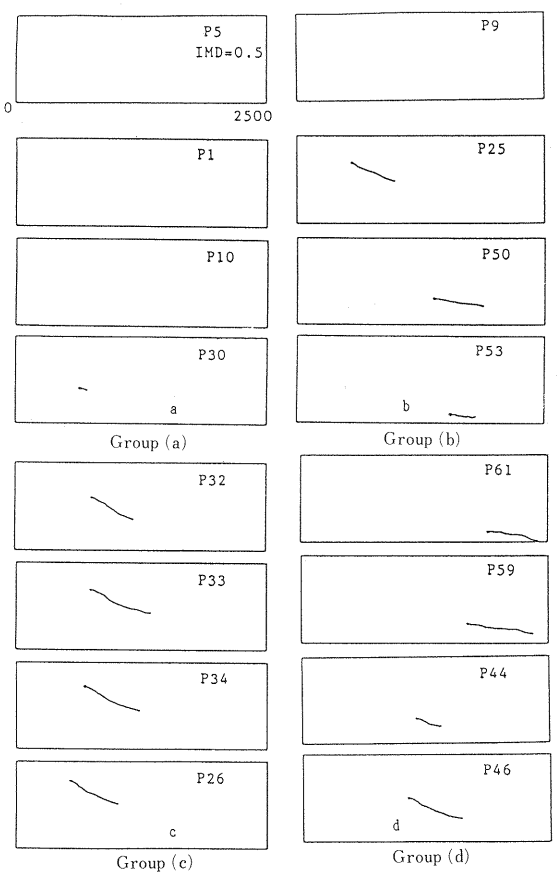

Fig. 20 Paths of 16 Particles Over a Period of 58 Seconds.

6. CONCLUDING REMARKS

On the basis of the results obtained from different numerical tests we conclude that

(1) The shape of the sliding section is wave like. This compares well with the actual phenomena observed after many earthquakes.

(2) The normal and shear force distributions make it possible to delineate the sliding area, which is in good agreement with the area defined by the velocity distributions.

(3) Large shear forces develop at the bottom of the assembly.

(4) Particle rotation has a major function in determining the sliding zone of a section.

ACKNOWLEDGEMENTS

We are grateful to Mr. Masahiro Iida (Research Associate, ERI) for his helpful suggestions and continuous encouragement throughout our investigation. All computations were done with the HITAC M 280 H (17.5 MFLOPS, 16 MB) computer at the Earthquake Research Institute.

REFERENCES

1) Ashida, K., Egashira, S. and Ohtsuki, H. : On the flow mechanism of sliding soil from a mountain slope, Bull. Disast. Prevention Res. Inst., Kyoto Univ. No. 26-B-2, pp. 315-327, 1982 (in Japanese).
2) Mogami, T. : A statistical approach to the mechanics of granular materials, Soils and Foundation, Vol. V, No. 2, 1965.
3) Cundall, P. A. : A computer model for simulating progressive, large scale movements in a blocky rock system, Symp. ISRM, Nancy, France, Proc. 2, pp. 129-136, 1971.
4) Cundall, P. A. and Strack, O. D. L. : A discrete numeral model for granular assemblies, Geotechnique, 29, No. 1, pp. 47-65, 1979.
5) Cundall, P. A., Drescher, A. and Strack, O. D. L. : Numerical experiments on granular assemblies; Measurements and observations IUTAM Conference on Deformation and Failure Granular Materials, Delft, 1982.
6) Kiyama, H., Fujimura, H. and Nishimura, T. : Ground surface settlement caused by tunnel excavation analyzed by the Cundall model, Anual Meeting of the Japan Society of Civil Engineers, 3, pp. 309-310, 1982 (in Japanese).
7) Kiyama, H. and Fujimura, H. : The gravity flow of granular assemblies of rock analyzed by the Cundall model, Proc. Japan Society of Civil Engineers, No. 333, pp. 137-146, 1983 (in Japanese).
8) Hakuno, M. and Hirao, T. : A trial related to random packing of particle assemblies, Proc. Japan Society of Civil Engineers, No. 219, pp. 55-63, 1973 (in Japanese).
9) Uemura, D. and Hakuno, M. : Granular assembly simulation for ground collapse, Bulletin of the Earthquake Research Institute, University of Tokyo. 62, pp. 19-59, 1987.
10) Uemura, D. and Hakuno, H : Granular assembly simulation with Cundall's model for the dynamic collapse of the foundation of a structure, Structural Eng./Earthquake Eng. Proc. of Japan Society of Civil Engineers 4, No. 1, pp. 155-164, 1987.

(Received April 19 1988)